ELSEVIER

Journal of Nuclear Materials 278 (2000) 251–257

journal of nuclear materials

www.elsevier.nl/locate/jnucmat

A model of the threshold stress intensity factor, K_{IH}, for delayed hydride cracking of Zr–2.5Nb alloy

Y.S. Kim *, Y.G. Matvienko [1], Y.M. Cheong, S.S. Kim, S.C. Kwon

Zirconium Team, Korea Atomic Energy Research Institute, P.O. Box 105, Yusong, Taejon 305-600, South Korea

Received 6 June 1999; accepted 24 September 1999

Abstract

An analytical model to predict a threshold stress intensity factor, K_{IH}, for delayed hydride cracking of Zr–2.5Nb alloy was developed based on a criterion to fracture hydrides: $\sigma^{A}_{max}(r_c) + \sigma^{h}(r_c) = \sigma^{h}_{f}$. The hydride platelet is assumed to cover a process zone ahead of the crack tip. By using the cohesive zone model and von Mises yield criterion at the boundary of the cohesive zone, the cohesive stress and the cohesive zone length (or the process zone length) were determined. The maximum stress and a critical distance in the process zone, corresponding to its occurrence, were obtained by assuming an elastic and linearly plastic materials with a constant tangent modulus, E_t. The feasibility of the developed K_{IH} model was discussed by comparing the predicted K_{IH} with the measured one by accounting for a temperature dependence of K_{IH}.

PACS: 62.20.M

1. Introduction

Delayed hydride cracking (DHC) of zirconium alloys is caused by diffusion of hydrogen (or deuterium) atoms to the vicinity of a crack tip, nucleation and growth of hydride platelets and fracture of the platelets. An initiation of DHC is controlled by the following two processes: the precipitation and growth of a hydride near the crack tip and a sufficiently high tensile stress enough to fracture it [1]. There are three kinds of initiation sites in zirconium alloys: a sharp crack or notch, a shallow and very smooth notch and a nominally smooth surface. However, a difference in defining stress fields at the three initiation sites will lead to different threshold parameters for crack initiation [2–9]. This study paid an attention to fracture initiation at a sharp crack.

The concept of fracture initiation at a sharp crack in zirconium alloys can be based on a local criterion of brittle fracture. The basic idea of the local criterion is that fracture occurs when the local stress reaches a critical value at a distance of $r = r_c$ ahead of the crack tip inside the process zone [10].

However, the question is how to define the maximum stress and the critical distance, r_c in the process zone and the length of the process zone. Shi [6] and Wappling [9] assume that the tensile stress remains constant as the maximum value in the process zone. Further, the critical distance, r_c, corresponding to the occurrence of the maximum stress, is assumed to be equal to two times the crack tip opening displacement, or 2δ for an elastic-perfectly plastic materials [6]. Besides, the hydride thickness is assumed to be constant independently of temperature even though the hydride thickness precipitated ahead of the crack tip increases with an increasing temperature [11]. As a result, there are some restrictions in predicting the threshold stress intensity factor, K_{IH}, leading to a disagreement between the measured and predicted K_{IH} values [6,9].

* Corresponding author. Tel.: +82-42 868 2359; fax: +82-42 868 8346.

E-mail address: yskiml@nanum.kaeri.re.kr (Y.S. Kim).

[1] Visiting scientist from the Department of Deformation and Fracture Mechanics, Mechanical Engineering Research Institute of the Russian Academy of Sciences, 4 M. Kharitonievsky Per., 101830 Moscow, Russia.

0022-3115/00/$ - see front matter
PII: S0022-3115(99)00249-4

The aim of this study is to develop an analytical model to predict the threshold stress intensity factor, K_{IH} for delayed hydride cracking of CANDU Zr–2.5Nb alloy. The process zone concept and cohesive zone model were used in this study to calculate the cohesive stress and the cohesive zone length by applying von Mises yield criterion at the zone boundary. The maximum stress and a critical distance in the process zone, corresponding to its occurrence, were determined by assuming an elastic and linearly plastic material with a constant tangent modulus, E_t.

2. Fracture criterion

A DHC process at the crack tip is associated with a crack tip stress field and the diffusion of hydrogen atoms to the vicinity of the crack tip inside the process zone. The hydrogen accumulation in the process zone leads to the precipitation of hydride platelets at the peak stress location ahead of the crack tip. However, the precipitation of hydrides accompanies compressive stresses in the matrix because of the increased volume of zirconium hydrides compared to that of metal zirconium [12–14]. Therefore, the tensile stress field ahead of the crack tip due to remotely applied stress and the compressive stress associated with hydride precipitation must be considered at the same time. In other words, a process zone ahead of the crack tip is determined by the applied stress as well as the compressive stress accompanied by the hydride precipitation.

Since no matrix ligament is experimentally observed between the crack tip and intact hydrides [11], it is reasonable to assume that the crack growth proceeds through fracturing of a hydride platelet precipitated at the crack tip. The hydride platelet of L long covers the process zone length, d due to $L \geqslant d$ (Fig. 1(a)). The remotely applied stress and the hydride precipitation process create a local stress within the hydride. It is also supposed that only the normal stress component of the local stress in the vicinity of the crack tip is active in the process zone. The local stress within the hydride is given by a linear superposition of two type of stresses: (a) $\sigma^A(r)$, normal to the crack plane, in the vicinity of the crack tip by an applied remote stress and (b) compressive stress, $\sigma^h(r)$, caused by the volume difference between zirconium and zirconium hydride. Hydrides fracture when the maximum superimposed stress of $\sigma^A(r)$ and $\sigma^h(r)$ is equal to a critical stress to initiate fracturing of hydrides, σ_f^h (Fig. 1(b)). Therefore, a local fracture criterion to fracture hydrides can be described as

$$\sigma_{max}^A(r_c) + \sigma^h(r_c) = \sigma_f^h. \tag{1}$$

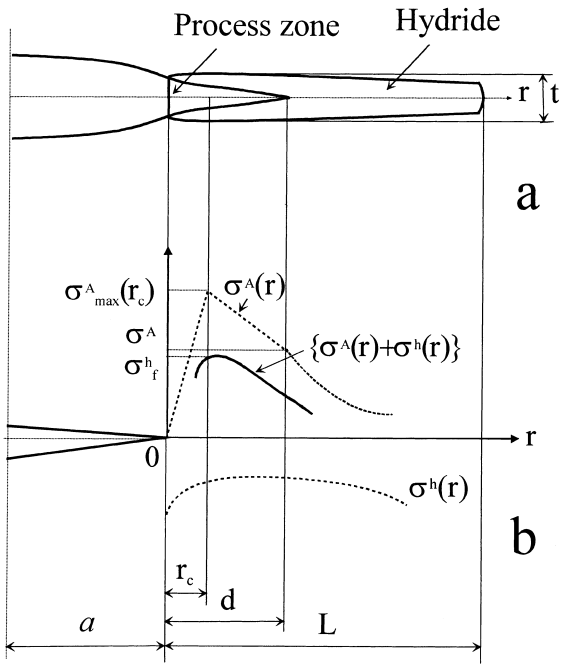

Fig. 1. Process zone model: (a) the hydride platelet of length L covering the process zone of length d; (b) the local stress distribution within the process zone.

2.1. Determination of σ_{coh} and the cohesive zone length, d

In an infinite plate with a crack length $2a$ under the applied tensile stress, the principal normal stresses on the crack extension line can be described (e.g., [15]):

$$\sigma_y(x) = \frac{\sigma x}{\sqrt{x^2 - a^2}}, \tag{2}$$

$$\sigma_x(x) = \sigma_y(x) - \sigma, \tag{3}$$

$$\sigma_z(x) = \begin{cases} v[\sigma_x(x) + \sigma_y(x)] & \text{(plane strain)}, \\ 0 & \text{(plane stress)}. \end{cases} \tag{4}$$

The crack opening displacement is given by a well-known expression

$$\delta = \frac{4\sigma}{E'}\sqrt{a^2 - x^2}, \tag{5}$$

where $E' = E$ for plane stress and $E' = E/(1 - v^2)$ for plane strain, E is the Young's modulus and v is Poisson's ratio and σ is the applied tensile stress.

To avoid the singularity of stress near the crack tip, it is assumed that the crack extends virtually from the actual crack tip at $x = a$ by the cohesive zone length d according to the Dugdale–Barenblatt type cohesive zone model (Fig. 2) [16,17]. Within this zone, the crack surfaces are loaded by the cohesive stress. For simplicity,

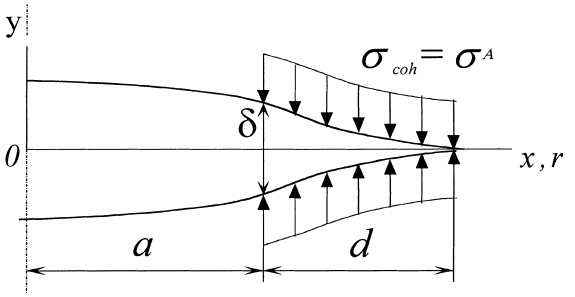

Fig. 2. The cohesive zone model ahead of the crack tip.

the cohesive stress is assumed to be constant. However, since the cohesive stress is associated with the discontinuity of materials, the cohesive zone length can be considered the same as the process zone length. Then, the cohesive zone length, d, was determined by putting the stress normal to the line of the virtual crack extension equal to the stress at the boundary of the cohesive zone (a criterion of border stress):

$$\sigma_y(x = d) = \sigma_{\mathrm{coh}}. \tag{6}$$

By combining Eqs. (2), (5) and (6), the cohesive zone length and the crack tip opening displacement (assuming a finite crack of $2a + 2d$ long) in an infinite plate with a finite crack was obtained:

$$d = \frac{K_{\mathrm{I}}^2}{\pi\sigma_{\mathrm{coh}}^2\left(\sigma/\sigma_{\mathrm{coh}}\right)^2}\left(\frac{1}{\sqrt{1-\left(\sigma/\sigma_{\mathrm{coh}}\right)^2}} - 1\right), \tag{7}$$

$$\delta = \frac{4\sigma}{E'}\sqrt{(a+d)^2 - a^2} = \frac{4K_{\mathrm{I}}}{E'}\sqrt{\frac{d}{\pi}\left(\frac{d}{a}+2\right)}, \tag{8}$$

where $K_{\mathrm{I}} = \sigma\sqrt{\pi a}$.

The cohesive stress was calculated by applying von Mises yield criterion at the boundary of the cohesive zone:

$$\Phi\left(\sigma_x, \sigma_y, \sigma_z, \sigma_Y\right) = \left(\sigma_x - \sigma_y\right)^2 + \left(\sigma_y - \sigma_z\right)^2 + \left(\sigma_z - \sigma_x\right)^2 - 2\sigma_Y^2 = 0. \tag{9}$$

Here, σ_{Y} is the yield stress, the stresses, σ_x and σ_z are given by Eqs. (3) and (4). From Eqs. (6) and (9), then σ_{coh} was determined as such

$$\sigma_{\mathrm{coh}} = \begin{cases} \frac{\sigma}{2} + \sigma_{\mathrm{Y}}\sqrt{\frac{1}{4}\left(\frac{\sigma}{\sigma_{\mathrm{Y}}}\right)^2 - \frac{(1+\nu^2-\nu)\ (\sigma/\sigma_{\mathrm{Y}})^2-1}{(1-2\nu)^2}} & \text{(plane strain)}, \\ \frac{\sigma}{2} + \sigma_{\mathrm{Y}}\sqrt{1 - \frac{3}{4}\left(\frac{\sigma}{\sigma_{\mathrm{Y}}}\right)^2} & \text{(plane stress)}. \end{cases} \tag{10}$$

2.2. Small scale yielding approximation and critical distance, r_c

The DHC process in zirconium alloys is associated with brittle fracture because critical applied stress is much smaller than the yield stress. In other words, the length of the cohesive zone (the inelastic region) is negligibly small compared to the crack length so that a small scale yielding approximation is valid. The condition $d/a \to 0$ is equivalent to $\sigma/\sigma_{\mathrm{coh}} \to 0$ ($\sigma/\sigma_{\mathrm{Y}} \to 0$). Thus, Eqs. (7) and (8) are reduced to as in the following, independent of the crack length:

$$d = \frac{K_{\mathrm{I}}^2}{2\pi\left(\sigma_{\mathrm{coh}}\right)^2}, \quad \delta = \frac{4}{\pi}\left(\frac{K_{\mathrm{I}}^2}{E'\sigma_{\mathrm{coh}}}\right). \tag{11}$$

Furthermore, as the yield stress becomes much greater than applied stress, i.e. when $\sigma/\sigma_{\mathrm{Y}} \to 0$, the cohesive stress shown in Eq. (10) is approximated as such

$$\sigma_{\mathrm{coh}} = \begin{cases} \sigma_{\mathrm{Y}}/(1-2\nu) & \text{(plane strain)}, \\ \sigma_{\mathrm{Y}} & \text{(plane stress)}. \end{cases} \tag{12}$$

A numerical analysis of the stress distribution at the crack tip shows that there is a maximum of the local stress at some distance away from the crack tip [15,18]. Furthermore, the presence of the maximum local stress has been confirmed experimentally by Leitch [19], who measured the elastic lattice strain of (0 0 0 2) plane ahead of the crack tip with time-neutron diffraction measurements. Since the cohesive stress must vanish at $r = 0$ and obey the boundary condition (6) for the cohesive zone, therefore, it is quite reasonable to assume that the cohesive stress is not kept constant but has a maximum somewhere in the cohesive zone. Furthermore, to simplify the calculation of the maximum stress and its location, we suggest that the cohesive stress linearly increases from zero to the maximum stress and decreases down to the cohesive stress, σ_{coh}, given by Eq. (12) as shown in Fig. 1. From the concept of force balance [20] and setting $\sigma_{\mathrm{coh}}(r) = \sigma^{\mathrm{A}}(r)$, the critical distance, r_{c}, was obtained as such

$$r_{\mathrm{c}} = \left(\frac{\sigma_{\max}^{\mathrm{A}}}{\sigma^{\mathrm{A}}} - 1\right)d. \tag{13}$$

2.3. Maximum stress, σ_{max}^A

To determine the ratio of $\sigma_{\max}^{\mathrm{A}}/\sigma^{\mathrm{A}}$, we consider the deformation behaviour of a hypothetically smooth microspecimen of unhydrided Zr–2.5Nb in the process zone. In this case, the ratio $\sigma_{\max}^{\mathrm{A}}/\sigma^{\mathrm{A}}$ could be expressed as the ratio of the ultimate tensile stress σ_{t} of the microspecimen situated at the point $r = r_{\mathrm{c}}$ to its yield stress. Since a DHC crack grows by fracturing of a hydride reprecipitated near the crack tip, it is assumed that the process zone ahead of the crack tip is covered

with the hydride. When the applied stress exceeds the ultimate tensile stress of the microspecimen, we assume that the hydride covering the microspecimen is fractured at the thickness, t, corresponding to the extended length of the microspecimen on the condition of $\sigma = \sigma_t$. As the microspecimen elongation corresponds to the threshold crack tip opening displacement, δ_{1H}, therefore, the strain, ε_t, corresponding to the stress σ_t, was approximated as the ratio of the threshold crack tip opening displacement δ_{1H} to the hydride thickness t for $\delta_{IH} < t$:

$$\varepsilon_t = \frac{\delta_{IH}}{t - \delta_{IH}} \approx \frac{\delta_{IH}}{t}.$$

The mechanical behaviour of the hypothetical microspecimen can be described by an uniaxial stress–strain curve of Zr–2.5Nb. If this material is assumed to behave elastic and linearly plastic with a tangent modulus E_t, the ultimate tensile stress can be described by

$$\sigma_t = \sigma_Y + (\varepsilon_t - \varepsilon_Y)E_t, \tag{14}$$

where $\varepsilon_Y = \sigma_Y/E$. Thus, the ratio σ^A_{max}/σ^A is represented as follows:

$$\frac{\sigma^A_{max}}{\sigma^A} = \frac{\sigma_t}{\sigma_Y} = 1 + \left(\frac{\delta}{t} - \varepsilon_Y\right)\frac{E_t}{\sigma_Y}. \tag{15}$$

A difference in the real stress state ahead of the crack tip and the hypothetical microspecimen under uniaxial tensile loading was ignored, since we consider the relative values of stress, σ^A_{max}/σ^A and σ_t/σ_Y. From Eqs. (11)–(13) and (15), the critical distance r_c was obtained:

$$r_c = \kappa d, \tag{16}$$

where κ is given by equations

$$\kappa = \left[\frac{4}{\pi}\frac{(1-\nu^2)\ (1-2\nu)K^2_{IH}}{\sigma^2_Y t} - 1\right]\frac{E_t}{E} \quad \text{(plane strain)} \tag{17}$$

and

$$\kappa = \left[\frac{4}{\pi}\frac{K^2_{IH}}{\sigma^2_Y t} - 1\right]\frac{E_t}{E} \quad \text{(plane stress)}. \tag{18}$$

Thus, σ^A_{max} stress becomes

$$\sigma^A_{max} = (1+\kappa)\sigma^A. \tag{19}$$

It is note that according to Eq. (19), the local maximum stress has a dependence on the yield stress, the threshold stress intensity factor, the thickness of the crack tip hydride and the ratio, E_t/E, as well.

2.4. Compressive stress caused by hydride precipitates

The stress within a hydride generated by the hydride precipitation in the absence of the applied stress can be calculated considering a representative simple geometry for hydride platelets. These platelets lie in, or close to, the crack plane. The hydride platelet only generates a stress free (transformation) strain normal to the disk-shaped platelet ($\varepsilon_\perp$) while all other components are zero. Thus, by using the equations suggested by Smith [21] and Shi [6], a simple expression for the compressive stress σ^h was obtained at larger values of r ($r > 0.25t$).

$$\sigma^h = -\frac{E\varepsilon_\perp}{4\pi(1-\nu^2)}\frac{t}{r}. \tag{20}$$

If the critical distance r_c does not satisfy the condition $r_c \geqslant 0.25t$, another equation for σ^h can be used by considering the free surface effect on σ^h at the crack tip region

$$\sigma^h = -\frac{E\varepsilon_\perp}{4\pi(1-\nu^2)}\frac{t}{r+\Delta t}, \tag{21}$$

where $\Delta = \frac{1}{2\pi}\exp(-6.518r/t)$ [6].

3. Prediction of K_{IH} for Zr–2.5Nb alloy

3.1. Threshold stress intensity factor

An expression for the threshold stress intensity factor, K_{IH}, was derived from the local fracture criterion Eq. (1) by putting Eqs. (11), (12), (16), (19) and (20) into the Eq. (1) and by setting $r = r_c$, $\sigma_{coh} = \sigma^A$

$$K^2_{IH} = \frac{E\sigma_Y\varepsilon_\perp t}{2\kappa(1-\nu^2)(1-2\nu)^2\left(\frac{1+\kappa}{1-2\nu} - \frac{\sigma^h_f}{\sigma_Y}\right)} \quad \text{(plane strain)}, \tag{22}$$

and

$$K^2_{IH} = \frac{E\sigma_Y\varepsilon_\perp t}{2\kappa\left(1+\kappa-\frac{\sigma^h_f}{\sigma_Y}\right)} \quad \text{(plane stress)}, \tag{23}$$

Eqs. (22) and (23) are transcendental equations, since the factor κ, given by Eqs. (17) and (18) for plane strain and plane stress, respectively, changes with K_{IH}.

In addition, a mixed plane condition is assumed in the process zone [9]. It is because fracturing of hydrides occurs in the process zone whose size is determined by a plane stress condition while the local stress in the process zone is supposed to be in the plane strain condition. In other words, while the process zone is formed in the plane stress condition due to applied stress, the precipitation and growth of hydrides in the process zone change the stress triaxiality to the plane strain condition at the point $r = r_c$. In this case, K_{1H} was expressed as such

$$K_{IH}^2 = \frac{E\sigma_Y\varepsilon_\perp t}{2\kappa(1-\nu^2)\left(\frac{1+\kappa}{1-2\nu}-\frac{\sigma_f^h}{\sigma_Y}\right)} \quad \text{(mixed plane condition)}, \tag{24}$$

where the factor κ is described by Eq. (18) for the plane stress condition. It is very important to note that a linear strain hardening in the plastic region has been considered in the model through the factor, κ.

3.2. Comparison of the predicted and measured K_{IH} for Zr–2.5Nb alloy

The threshold stress intensity factors, K_{IH}, of Zr–2.5Nb alloy were calculated using Eqs. (22)–(24). Here, the assumptions used in the calculation are $E_t/E = 0.01$ and the transformation strain, $\varepsilon_\perp$, of about 0.17 [13] while other mechanical constants used in the calculations are given in Table 1.

Assuming a constant hydride thickness of $t = 2$ μm, the calculated threshold stress intensity factor, K_{IH}, decreased with an increasing temperature as shown in Table 2, which is quite opposite to the measured temperature dependence of K_{IH} [6]. The reason for a large disagreement between calculated and measured K_{IH} values could be attributed to a constant hydride thickness independent of temperature.

Shek has reported that the length and thickness of hydrides increase with an increasing DHC temperature [11]. Therefore, the temperature dependence of hydride thickness must be included into the equations describing the threshold stress intensity factor. Unfortunately, to our knowledge, there is a limited number of measurements reported in literature that directly determines the change in the hydride thickness with temperature in Zr–2.5Nb alloy.

Table 1
Mechanical properties for Zr–2.5Nb [6]

E	$= 95900 - 57.4[T(\mathrm{K}) - 273]$ (MPa)
ν	$= 0.436 - 4.8 \times 10^{-4}[T(\mathrm{K}) - 300]$
σ_Y	$= 1088 - 1.02T(\mathrm{K})$ (MPa)
σ_f^h	$= 7.357 \times 10^{-3}E$

From a strain of the microspecimen ahead of the crack tip, the hydride thickness can be related to the threshold crack opening displacement, δ_{1H} at the moment of the crack initiation. From Eq. (11), the hydride thickness was expressed as such

$$t = \frac{\delta_{1H}}{\varepsilon_t} = \beta\left(\frac{1}{E'\sigma^A}\right) \quad \text{here } \beta = \frac{4K_{IH}^2}{\pi\varepsilon_t}. \tag{25}$$

It is assumed that β changes little with temperature. Then, Eq. (25) suggests that the hydride thickness increases with decreasing yield stress and Young's modulus or with an increasing temperature. Fig. 3 shows a change of the hydride thickness with temperature in the plane strain and plane stress conditions. By putting the hydride thickness variation with temperature (as shown in Fig. 3) into Eqs. (22)–(24), K_{1H} was calculated again as shown in Table 3. The largest K_{1H} values were still obtained from the plane strain condition as opposed to other conditions. Furthermore, the temperature dependence of K_{1H} did not appear neither in the plane stress nor plane strain conditions. In contrast, the calculated K_{1H} in the mixed condition shows an increasing trend with an increasing temperature, whose values seem to be a bit lower than the measured K_{1H}. In other words, the temperature dependence of K_{1H} is best described by Eq. (24) only in the mixed condition.

There are at least a few factors that could affect the theoretical estimation of the threshold stress intensity factor. One thing is to account for the temperature effect of the ratio E_t/E. Another thing is the coverage of hydrides ahead of the crack tip. It is assumed that a single hydride platelet covers the process zone up to now. However, considering the formation of multi-layered hydrides in the process zone and possibly uneven

Table 2
The calculated $K_{IH}(\mathrm{MPa}\sqrt{m})$ value of unirradiated Zr–2.5Nb with the constant hydride thickenss of $t = 2$ μm

Temperature (K)	Plane condition model		
	Plane strain	Plane stress	Mixed plane condition
350	14.1	6.4	3.8
500	8.5	5.3	3.6

Table 3
The calculated K_{IH} ($\mathrm{MPa}\sqrt{m}$) of unirradiated Zr–2.5Nb with a variable hydride thickness with temperature as shown in Eq. (25)[a]

Temperature (K)	Plane condition model		
	Plane strain	Plane stress	Mixed plane condition
350	12.4	7.9	4.7
500	12.3	7.8	5.3

[a] A mean experimental range of K_{IH} values is 6 to 8 $\mathrm{MPa}\sqrt{m}$ at temperatures ranging from 350 to 500 K [6].

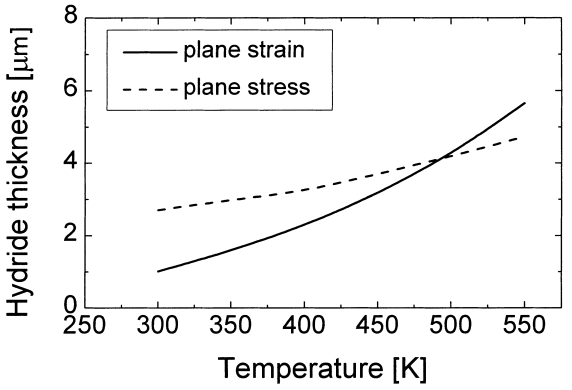

Fig. 3. Temperature dependence of the hydride thickness precipitated in the process zone of unirradiated Zr–2.5Nb alloys for various stress state conditions.

coverage of hydrides across and along the front of the crack tip [6,9], the predicted value of K_{IH} could become larger

$$K_{IH} = fK_{IH}^{s} + (1-f)K_{Ic}^{Zr}. \tag{26}$$

Here, f is the fraction of hydride coverage ahead of the crack tip, K_{IH}^{s} is the threshold stress intensity factor with the coverage of a single hydride platelet, which was derived from Eq. (24) and $K_{Ic}^{Zr} = 30 + 0.045(T - 300)$ (MPa$\sqrt{m}$) [9] for fracture toughness of CANDU Zr–2.5Nb alloy containing hydrides. Fig. 4 shows a comparison of theoretically predicted K_{IH} values (Eqs. (24) and (26)) and the measured ones as a function of temperature with f varying from 0.9 to 1.0. Here, all the measured threshold stress intensity factors reported by Shi [6] and Sagat [22] were put together for the temperatures ranging from 350 to 600 K to clearly find out the temperature dependence of the measured K_{IH}.

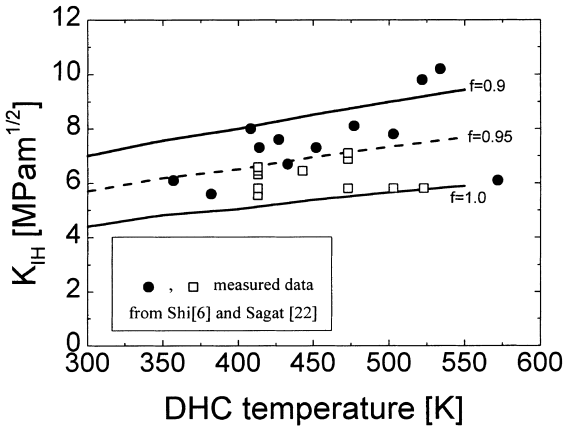

Fig. 4. Comparison of the predicted threshold stress intensity factors (Eq. (24)) of unirradiated Zr–2.5Nb and the measured ones with the area fraction, f, of hydride coverage in front of the crack tip ranging from 0.9 to 1.

The predicted K_{IH} values are weakly dependent on temperature and correspond quite well to the measured K_{IH} values. The temperature tendency of K_{IH} in the developed model could arise mostly from the temperature dependence of the hydride thickness and the maximum local stress within the process zone associated with the value of $(1+k)/(1-2v) - \sigma_f^h/\sigma_Y$. This is in contrast to Shi's model [6] that poorly predicts the temperature dependence of the measured K_{IH} by assuming the constant local stress with the process zone and constant hydride thickness independent of temperature. It is to note that the temperature effect of the ratio, E_t/E, on K_{IH} has not been taken into account for the present calculation. Nevertheless, the predicted K_{IH} is qualitatively consistent with the measured data, while the predicted K_{IH} with the coverage of a single hydride ($f = 1$) represents the lower bound of the experimentally measured K_{IH}.

4. Conclusions

An analytical model to predict K_{IH} for delayed hydride cracking of CANDU Zr–2.5Nb alloy was developed based on a local fracture criterion. The hydride platelet is assumed to cover a process zone ahead of the crack tip. By using a cohesive zone model and von Mises yield criterion at the boundary of the cohesive zone, the cohesive stress and the cohesive zone length (or the process zone length) were determined. The maximum stress and a critical distance in the process zone, corresponding to its occurrence, were obtained by assuming elastic and linearly plastic materials with a constant tangent modulus, E_t. Depending on the stress state ahead the crack tip, three different kinds of predicted K_{IH} values were obtained for a plane stress condition, plane strain condition and mixed plane condition. Comparison of the predicted and measured K_{IH} values shows that the predicted K_{IH} in the mixed plane condition covers the lower bound of the measured K_{IH} values with a gradual increase of hydride thickness with temperature. By introducing a fraction of hydride coverage ahead of the crack tip in the process zone, a qualitatively good agreement between the predicted and measured K_{IH} values was obtained.

Acknowledgements

This work has been carried out as a part of the Nuclear R&D program supported by Ministry of Science and Technology, Korea. In addition, additional financial support by Korea Institute of Science and Technology, Evaluation and Planning is acknowledged.

References

[1] M.P. Puls, Nucl. Eng. Des. 171 (1997) 137.
[2] E. Smith, Int. J. Press. Vessels Piping 60 (1994) 159.
[3] X.J. Zheng, L. Luo, D.R. Metzger, R.G. Sauve, J. Nucl. Mater. 218 (1995) 174.
[4] S.Q. Shi, M.P. Puls, S. Sagat, J. Nucl. Mater. 208 (1994) 243.
[5] E. Smith, Int. J. Press. Vessels Piping 68 (1996) 53.
[6] S.Q. Shi, M.P. Puls, J. Nucl. Mater. 208 (1994) 232.
[7] E. Smith, Int. J. Press. Vessels Piping 61 (1995) 1.
[8] K.S. Chan, J. Nucl. Mater. 227 (1996) 220.
[9] D. Wappling, A.R. Massih, P. Stahle, J. Nucl. Mater. 249 (1997) 231.
[10] R.O. Ritchie, R.O. Knott, J.R. Rice, J. Mech. Phys. Solids 21 (1973) 395.
[11] G.K. Shek, M.T. Jovanovic, H. Seahra, Y. Ma, D. Li, R.L. Eadie, J. Nucl. Mater. 231 (1996) 221.
[12] L.A. Simpson, M.P. Puls, Metall. Trans. A10 (1979) 1093.
[13] R.L. Eadie, F. Ellyin, Scripta Metall. 23 (1989) 585.
[14] G.C. Weatherly, Acta Metall. 29 (1981) 501.
[15] T.L. Anderson, Fracture Mechanics: Fundamentals and Applications, CRC Press, Boca Raton, 1995.
[16] D.S. Dugdale, J. Mech. Phys. Solids 8 (1960) 100.
[17] G.I. Barenblatt, Adv. Appl. Mech. 7 (1962) 55.
[18] R.M. McMeeking, J. Mech. Phys. Solids 25 (1977) 357.
[19] B. Leitch, N. Christodoulou, J. Root, in: Transactions of the 15th International Conference on Structural Mechanics in Reactor Technology, 1999, p. XII–133.
[20] Yu.G. Matvienko, Int. J. Fract. 1999 (in press).
[21] E. Smith, J. Mater. Sci. 29 (1994) 1121.
[22] S. Sagat, C.E. Coleman, M. Griffiths, B.J.S. Wilkins, in: A.M. Garde, E.R Bradley (Eds.), Zirconium in the Nuclear Industry: 10th International Symposium, ASTM STP 1245, American Society for Testing Materials, Philadelphia, 1994, p. 35.